Supplementary material

Modulation of the stability of the *Salmonella* fourU-type RNA thermometer

Jörg Rinnenthal[1], Birgit Klinkert[2], Franz Narberhaus[2] and Harald Schwalbe[1]*

[1]Institute for Organic Chemistry and Chemical Biology, Center for Biomolecular Magnetic Resonance, Johann Wolfgang Goethe-University, Max-von-Laue-Strasse 7, D-60438 Frankfurt/Main, Germany.

[2]Microbial Biology, Ruhr-Universität Bochum, Universitätsstrasse 150, NDEF06/783, 44780 Bochum, Germany.

E-mail: schwalbe@nmr.uni-frankfurt.de

CD unfolding and refolding curves

CD unfolding and refolding curves of the wt (Figure S1), A8C-mutant (Figure S2) and G14A-C25U-mutant (Figure S3) were analyzed to investigate the reversibility of the global unfolding process. All three RNAs show unfolding and refolding curves that are very similar indicating that the unfolded RNA is able to refold to its native fold under the given buffer conditions (15 mM $K_xH_yPO_4$, pH 6.5, 25 mM KCl). However, unfolding and refolding curves are slightly shifted. This shift is due to incomplete equilibration of the RNA at the given temperature since the shift is dependent on the temperature slope used in the temperature scan. For the analysis of the melting point T_m and the extraction of the thermodynamic parameters of the global unfolding transition ΔG_{unf}, ΔH_{unf} and ΔS_{unf} unfolding and refolding curves were averaged.

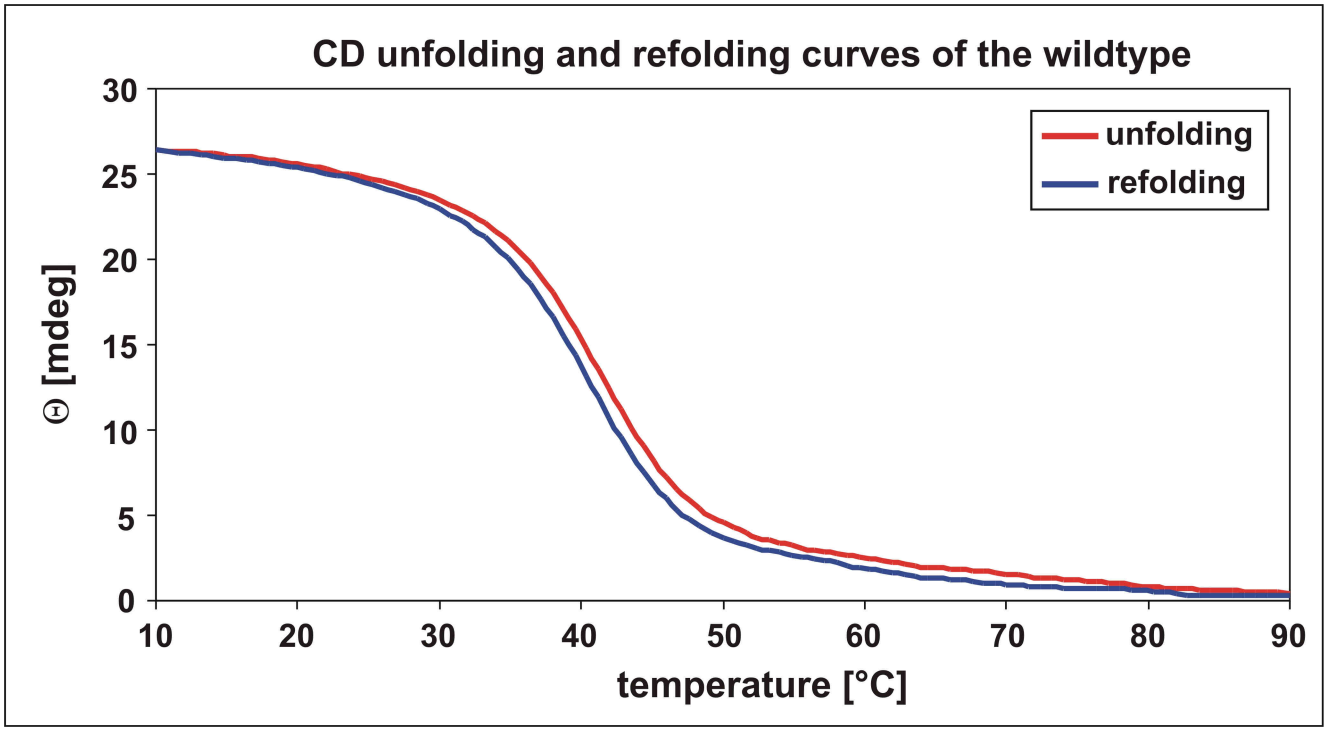

Figure S1: CD unfolding (red line) and refolding (blue line) curves of the 4U-hp2-wt RNA recorded at a wavelength of 258 nm with a temperature slope of 1°C/min and -1°C/min for unfolding and refolding, respectively.

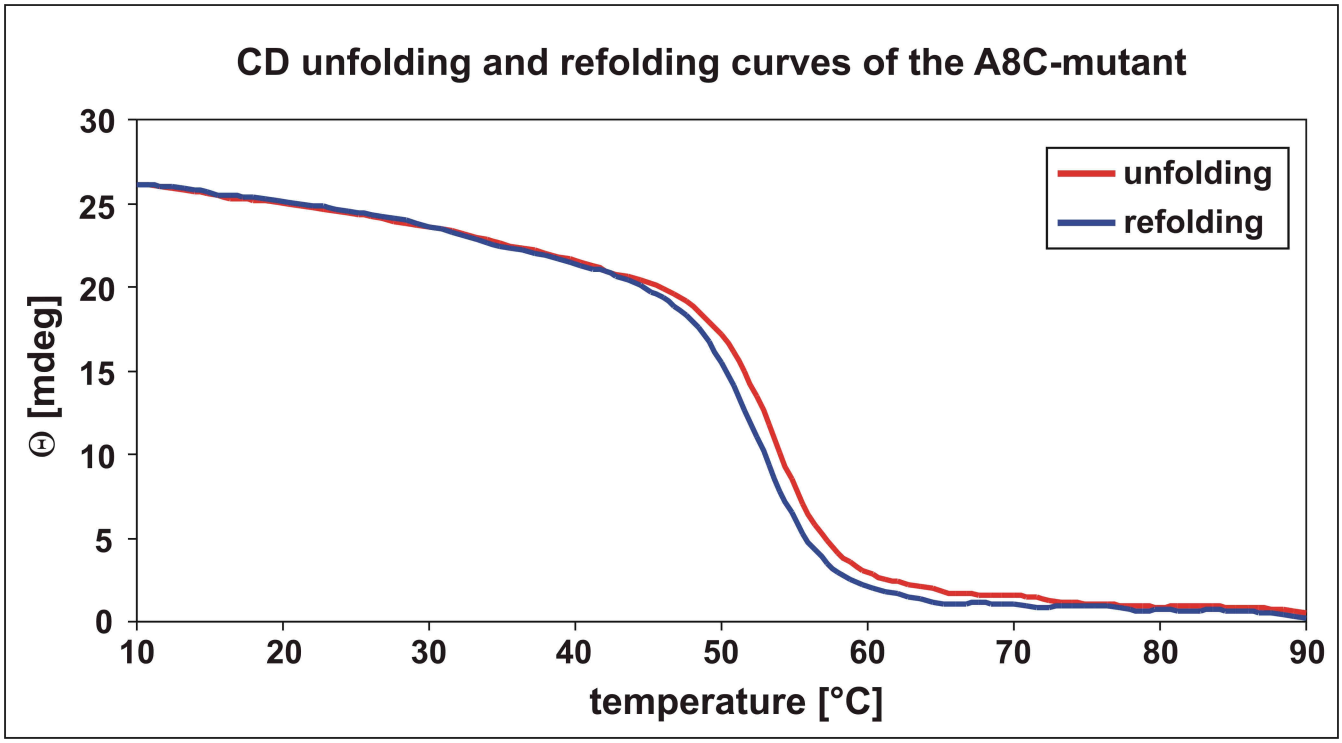

Figure S2: CD unfolding (red line) and refolding (blue line) curves of the 4U-hp2-A8C-mutant RNA recorded at a wavelength of 258 nm with a temperature slope of 1°C/min and -1°C/min for unfolding and refolding, respectively.

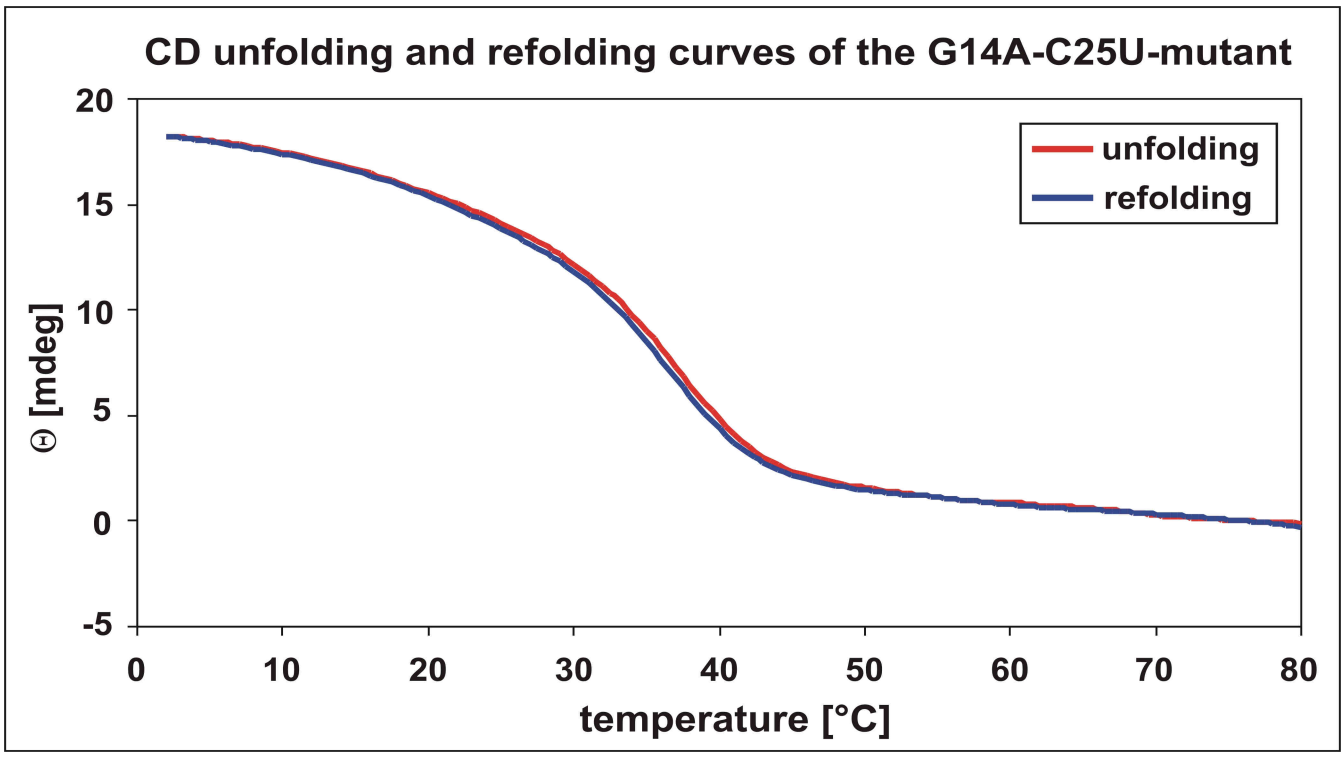

Figure S3: CD unfolding (red line) and refolding (blue line) curves of the 4U-hp2-G14A-C25U-mutant RNA recorded at a wavelength of 258 nm with a temperature slope of 1°C/min and -1°C/min for unfolding and refolding, respectively.

Monophasic CSP fitting results of the imino resonances of the 4U-hp2-wt RNA

Mg^{2+} titrations of the 4U-hp2-wt RNA were performed and the resulting CSP curves of the imino group resonances were fitted as described (main article, materials and methods, Mg^{2+} titration experiments). Table S1 illustrates the values for the respective maximum CSP and dissociation constant K_{diss} for each analyzed imino signal obtained from the monophasic fit according to equation (2) (main article).

Table S1: CSPs of the imino groups of the nucleobases of the 4U-hp2-wt RNA caused by the addition of $MgCl_2$. CSP_{max} and K_{diss}-values were derived by fitting of the CSP curves by equation (2) (main article). CSP_{max}: CSP at infinite Mg^{2+}-concentration; K_{diss}: dissociation constant.

	CSP_{max} [ppm]	**K_{diss} [mM]**
U4	0.057 ± 0.003	0.85 ± 0.18
U5	0.119 ± 0.004	2.51 ± 0.19
G6	0.045 ± 0.002	2.12 ± 0.21
U33	./.[c]	./.[c]
U32	./.[a]	./.[a]
G30	./.[a]	./.[a]
U10	./.[b]	./.[b]
U11	./.[b]	./.[b]
G27/G28	./.[c]	./.[c]
U12	./.[c]	./.[c]
U13	0.250 ± 0.008	2.38 ± 0.16
G14	0.030 ± 0.001	1.17 ± 0.12
U24	0.045 ± 0.003	3.77 ± 0.42
U23	0.085 ± 0.005	3.34 ± 0.36

a: imino signal too weak or not detectable b: no CSP c: no valid fit

Cooperativity of the two Mg^{2+} binding sites

According to the CSP curves, the 4U-hp2-wt RNA has two distinct Mg^{2+} binding sites. Binding of the Mg^{2+} ions shows positive cooperative effects. These effects can be quantified by the Hill coefficient. To quantify the extent of cooperativity the fraction of occupied Mg^{2+} binding sites as a function of the Mg^{2+} concentration was simulated according to the determined macroscopic dissociation constants K_1 and K_2 (Table 3, main article). Subsequently, the $\theta([Mg^{2+}])$ curve was fitted according to a four parameter Hill equation (equation S1).

$$\boldsymbol{\theta}([\boldsymbol{Mg}^{2+}]) = \boldsymbol{y}0 + \frac{\boldsymbol{a} * [\boldsymbol{Mg}^{2+}]^{\boldsymbol{b}}}{\boldsymbol{c}^{\boldsymbol{b}} + [\boldsymbol{Mg}^{2+}]^{\boldsymbol{b}}} \qquad \text{(S1)}$$

In equation (S1) $\theta([Mg^{2+}])$ is the fraction of occupied Mg^{2+} binding sites, y0 is the ordinate intercept, a is the amplitude, c the concentration at which 50% of the Mg^{2+} binding sites are occupied and b is the Hill coefficient.

The simulated $\theta([Mg^{2+}])$ curve and the sigmoidal fit are illustrated in Figure S4. Apparently, the simulated curve can be fitted by equation (S1). The extracted Hill coefficient is equal to b=1.47. For RNA molecules with two Mg^{2+} binding sites the Hill coefficient has to be in the range between 1-2. A factor b=1 indicates uncooperative binding while b=2 indicates maximum cooperativity. Factors of b<1 indicate negative cooperativity. Apparently, the observed b factor is directly in between uncooperative binding and maximum cooperativity. Thus, the two Mg^{2+} binding sites of the 4U-hp2-wt RNA exhibit intermediate cooperativity.

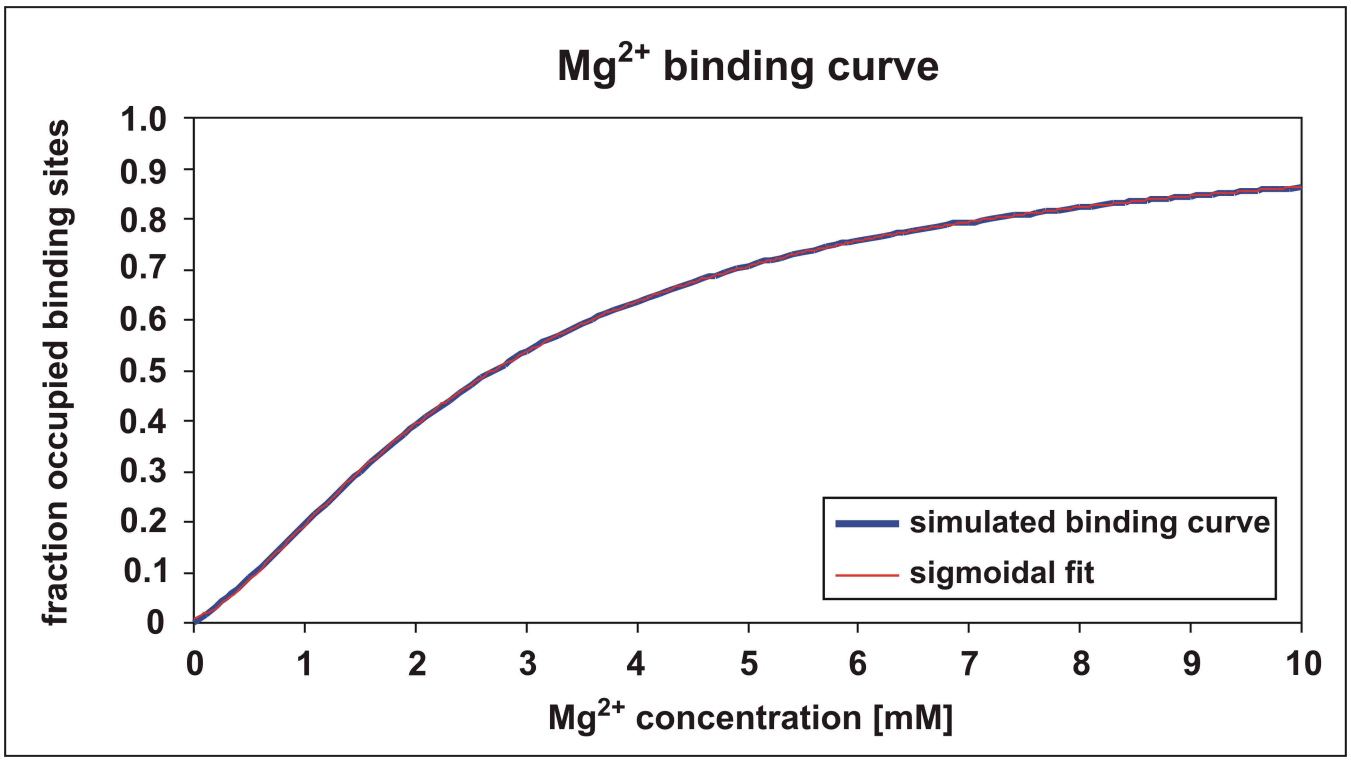

Figure S4: Plot of the fraction of occupied Mg^{2+} binding sites in the 4U-hp2-wt RNA versus the Mg^{2+} concentration. Parameters used for the simulated curve (blue line): K_1 = 3.58 mM, K_2 = 2.06 mM. The simulated curve was fitted according to a four parameter Hill equation (red line).

Mg^{2+} binding model for one binding site but different conformations of the [RNA*Mg^{2+}] complex

A Mg^{2+} binding model assuming an [RNA*Mg^{2+}]-complex with only one Mg^{2+} binding site but three different Mg^{2+} bound states is given in Figure S5.

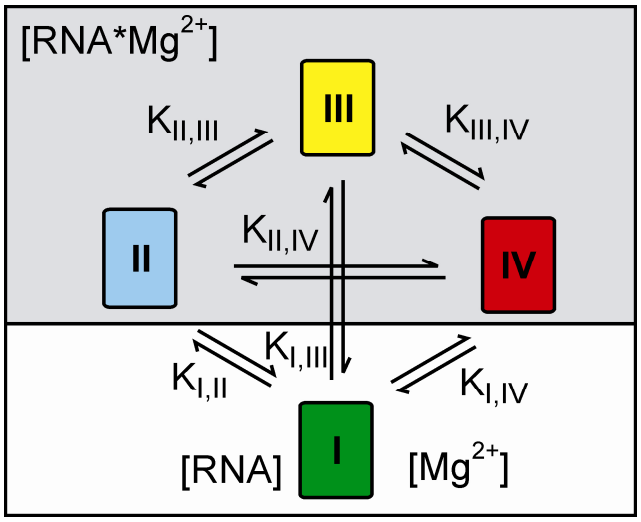

Figure S5: Mg^{2+} binding model assuming one single Mg^{2+} binding site but three different conformations of the [RNA*Mg^{2+}] complex. In this model, the free form in indicated as I (green) and the three different [RNA*Mg2+] complexes are indicated as II (blue), III (yellow) and IV (red).

In this model (Figure S5), the free form of the RNA is in equilibrium with the three different Mg^{2+}-bound forms (II, III, IV). The Mg^{2+}-bound forms [II, III and IV] are either directly connected to each other or via the free form of the RNA so that the complexes II, III, and IV are in equilibrium to each other, too. The equilibria can be described by the following equations:

$$K_{II,III} = [III]/[II] \quad \text{(S2)}$$

$$K_{II,IV} = [IV]/[II] \quad \text{(S3)}$$

$$K_{III,IV} = [IV]/[III] \quad \text{(S4)}$$

Note that the equilibria in the equations S2, S3 and S4 are not dependent on the Mg^{2+} concentration. In contrast, the equilibria of the state I with the states II, III and IV (equations (S5), (S6) and (S7)) are dependent on the Mg^{2+} concentration.

$$K_{I,II} = \frac{[I][Mg^{2+}]}{[II]} \quad \text{(S5)}$$

$$K_{I,III} = \frac{[I]/[Mg^{2+}]}{[III]} \quad \text{(S6)}$$

$$K_{I,IV} = \frac{[I][Mg^{2+}]}{[IV]} \quad \text{(S7)}$$

Insertion of the equations (S2) and (S3) into the equations (S6) and (S7) leads to equation (S8)

$$K_{I,II} = K_{I,III} * K_{II,III} = K_{I,IV} * K_{II,IV} = \frac{[I][Mg^{2+}]}{[II]} \quad \text{(S8)}$$

From equation (S8) a monophasic hyperbolic binding curve can be deduced. Thus, the binding model in Figure S5 leads to monophasic and hyperbolic CSP curves with the same apparent binding constant for all curves.

Significantly varying K_{diss} values for different imino signals (Figure 8, main article; Table S1) and the biphasic CSP curve of nucleotide U12 (Figure 8, main article) cannot be explained by a model assuming only one Mg^{2+} binding site but different conformations for the [RNA*Mg^{2+}] complex (Figure S5).

Evidence for defined Mg^{2+} binding

The Mg^{2+} dependence of the melting point T_m is described in the main manuscript (Figure 5, Table 2). In Figure 5, the T_m values are plotted against the Mg^{2+} concentration and the free energy values for Mg^{2+} binding are derived from the hyperbolic fit according to equation (14).

The same data can also be plotted differently. According to (1,2) a plot of ($1/T_m$) against ln[Mg^{2+}] should be sigmoidal in case of diffuse binding but should reveal a linear dependency in case of specific Mg^{2+} binding. The corresponding plot is given in Figure S6.

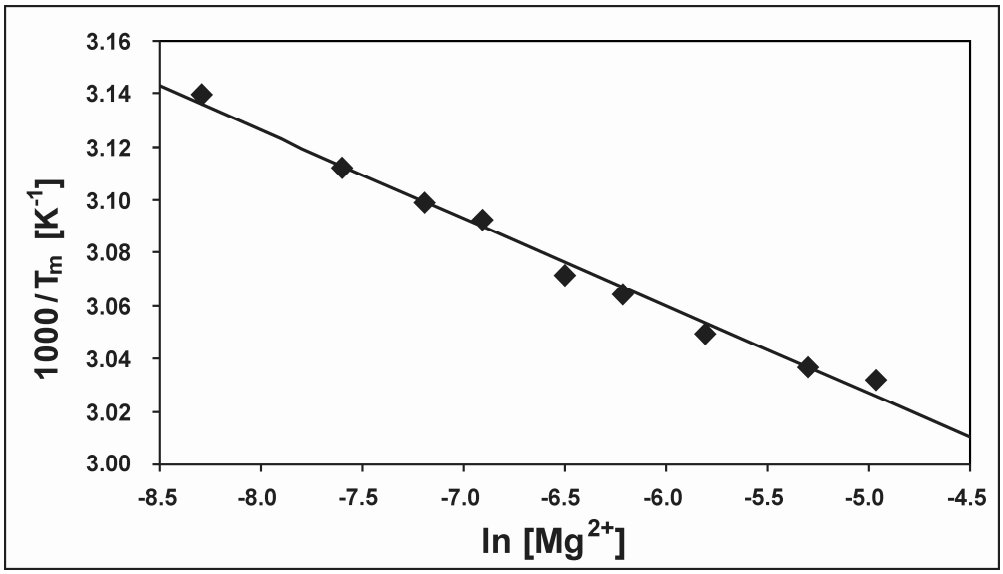

Figure S6 ($1/T_m$) on ln[Mg^{2+}] dependence of the 4U-hp2-wt RNA as derived from CD melting curves. The curve can be fitted linearly according to the equation f = y0 + mx. Fitting results are y0 = $2.8612*10^{-3} \pm 8.62*10^{-6}$, m = $3.3126*10^{-5} \pm 0.1304*10^{-5}$ and $r^2 = 0.9893$.

Apparently, the plot in Figure S6 reveals a linear dependency. Therefore, the observed Mg^{2+} dependence of T_m is caused by specific Mg^{2+} binding. Consequently, the CSP curves of the imino region (Figure 8, main article) are caused by specific Mg^{2+} binding. The plot of 1/Tm vs. ln[Mg^{2+}] would exhibit a superposition of a sigmoidal curve for diffuse binding and a linear curve for defined binding, if diffuse

binding effects would cause significant T_m variations. According to Figure S6 the plot is purely linear and does not show any sigmoidal curvature in the concentration range investigated. Thus, the effects of specific Mg^{2+} binding clearly dominate over diffuse binding effects, at least in the concentration range (0-7mM) observed here.

Qualitative explanation of the observed CSP curves using a two binding site model

The different monophasic CSP curves can be described by a model with two Mg^{2+} binding sites (Figure 1, main article) as follows. While some imino groups sense the binding of a Mg^{2+} ion to the first binding site, other imino groups experience a CSP upon binding of a Mg^{2+} ion to the second binding site. A few imino signals might sense only the formation of the binary or only the formation of the ternary complex, others might experience different CSPs for the different Mg^{2+} binding sites. Due to the observed cooperativity, the model predicts two dissociation constants for a particular Mg^{2+} binding site which lead to two superimposing curves. However, the respective dissociation constants ($K_{2,4}$; $K_{1,2}$) are very different so that only the small dissociation constant $K_{2,4}$ is observable. The same is true for the second Mg^{2+} binding site (dissociation constants $K_{3,4}$; $K_{1,3}$) where only $K_{3,4}$ is observable. The signals U23 and U24 exhibit a dissociation constant of approximately 3.56 mM, which is within the margin of error of the macroscopic dissociation constant K_1. Thus, a scenario, in which U23 and U24 experience the transition between free RNA and binary complex, no matter which binding site is occupied, but do not exhibit a CSP upon transition between binary and ternary complex might explain the observed CSP curves. Monophasic CSP curves that show dissociation constants between 2.12 mM and 2.51 mM (G6, U13, U5) might result from overlapping biphasic CSP curves with equal signs for the CSPs of both transitions. Such curves might appear as monophasic curves with dissociation constants between K_1 (3.58 mM) and K_2 (2.06 mM), which is the case for G6 (2.12 mM), U13 (2.38 mM) and U5 (2.51 mM).

Literature

1. Laing, L.G., Gluick, T.C. and Draper, D.E. (1994) Stabilization of RNA Structure by Mg Ions - Specific and Nonspecific Effects. *Journal of molecular biology*, **237**, 577-587.

2. Misra, V.K. and Draper, D.E. (1998) On the role of magnesium ions in RNA stability. *Biopolymers*, **48**, 113-135.